

Conformation and Rigidity of DNA Microcircles Containing *waf1* Response Element for p53 Regulatory Protein

Haijun Zhou¹, Yang Zhang¹, Zhong-can Ou-Yang¹, Stuart M. Lindsay², Xi-Z. Feng^{2,3}, Pichumani Balagurumorthy³ and Rodney E. Harrington^{3*}

¹*Institute of Theoretical Physics, The Chinese Academy of Sciences, P.O. Box 2735, Beijing 100080, China*

²*Department of Physics and Astronomy, Arizona State University, Tempe AZ 85287, USA*

³*Department of Microbiology Arizona State University Tempe, AZ 85287, USA*

The tumor-suppressor activity of p53 is closely related to its DNA-binding properties. It binds a number of DNA response-elements and it is likely that these share a common structural feature. Here, we present a new, general method to determine the absolute twist of flexible DNA promoter sequences based on direct imaging of the topology of microcircles containing the sequences. We have used magnetically driven dynamic force microscopy ("MacMode" AFM) to observe, in solution, the conformation of 168 base-pair DNA microcircles, each containing four equally spaced copies of the *waf1/cip1/p21* p53 response-element. Analysis of the images showed that the microcircles are markedly puckered with a small excess of negatively writhed molecules. The average measured values of writhe are 0.109 ± 0.013 (for 60 positively writhed molecules) and -0.098 ± 0.011 (for 65 negatively writhed molecules). These values lead directly to a difference in linking number for the positively and negatively writhed molecules prior to ligation, from which we derive a twist mismatch of 178° (overtwist). This is 44.5° for each 42-mer precursor containing a single *waf1/cip1/p21* p53 response-element, in good agreement with the range of values deduced by indirect biochemical techniques. The two values of writhe may also be used to determine the ratio of the bending (*B*) to twisting (*C*) rigidity, yielding $B/C = 0.23$. This is about one-third of the value for long, random-sequence DNA, suggesting that the *waf1/cip1/p21* p53 response-element is extremely flexible, a result that is also consistent with indirect biochemical experiments. These results support the idea, proposed by us earlier, that torsional stress may play a role in the regulation of p53 binding through modulation of twist at the binding site.

© 2001 Academic Press

Keywords: p53; *waf1* DNA response-element; DNA microcircle; MacMode atomic force microscopy; writhe

*Corresponding author

Abbreviations used: p53, human wild-type tumor-suppressor protein; p53DBD, the minimal core DNA binding domain of human wild-type p53 encompassing amino acid residues 96-308; MacMode, magnetic alternating current mode; AFM, atomic force microscopy; APM, atomic probe microscope; APTES or AP, 3-aminopropyltriethoxysilane.

E-mail address of the corresponding author: harring@asu.edu

Introduction

p53 is a 53 kDa nuclear phosphoprotein known to be involved in cell-cycle regulation. In response to DNA damage, it brings about either cell-cycle arrest at G1/S phase or apoptosis through a cascade of events. These events rely primarily on the ability of p53 to function as a transcription factor, which in turn is closely tied with its DNA-binding properties. It has also been shown to possess tumor-suppressor activity in a large number of human cancers. (p53 has been reviewed by Ko & Prives, 1996; Levine, 1997; Ding & Fisher, 1998.)

p53 binds to DNA predominantly as a tetramer (Friedman *et al.*, 1993; Pavletich *et al.*, 1993; Stenger *et al.*, 1994). Wild-type p53 has three major functional domains (Pavletich *et al.*, 1993), the C-terminal tetramerization domain, the N-terminal transactivation domain and the central DNA-binding domain (p53DBD), in addition to linkage regions connecting these and a 30-residue basic C terminus which is known to modulate DNA-binding by the protein. The majority of human tumorigenic mutations occur in the central DNA-binding domain of p53 and may affect contacts between p53 and the DNA target or alter the structure of the DNA-binding domain. In either case, they abrogate or modulate the ability of p53 to bind DNA (Cho *et al.*, 1994).

Most of the p53 response-elements identified in the human genome are 20 base-pairs in length, containing two decameric half sites, following the consensus pattern RRRC(A/t)|(T/a)YYY, where R and Y denote purine and pyrimidine bases respectively, and the vertical bar indicates the center of pseudodyad symmetry (Kern *et al.*, 1991; El-Deiry *et al.*, 1992; Tokino *et al.*, 1994). Recent studies have found that in addition to protein-DNA contacts, the deformability of the p53 DNA response-elements contributes significantly to the selective binding of p53 to the DNA and the DNA bend in the p53-DNA complex is essential for its stability (Balagurumorthy *et al.*, 1995; Nagaich *et al.*, 1997a,b, 1999; Cherny *et al.*, 1999; Jett *et al.*, 2000).

In order to reduce the energetic cost involved in p53-induced DNA bending, we have hypothesized that the DNA response-elements must be anisotropically flexible (Durell *et al.*, 1998). Inspection of several functional p53 response-elements has led to the suggestion that the highly conserved tetranucleotide sequence d(CATG.CATG) at the pseudodyad junction in the half sites could be the sites of such anisotropic flexibility. The flexibility of d(CA.TG) sequences is well documented and has been shown to be the origin of DNA bending observed in the structures of many nucleoprotein complexes (McNamara *et al.*, 1990; Steitz, 1990; Schultz *et al.*, 1991; Harrington, 1992, 1993; Nagaich *et al.*, 1994; ElHassan & Calladine, 1996; Werner *et al.*, 1996; Bewley *et al.*, 1998; Olson *et al.*, 1998). The remarkable ability of the d(CATG.-CATG) sequence to roll either into a major or minor groove is the basis for the molecular model developed for tetrameric p53 bound to the *waf1/cip1/p21* response-element (Nagaich *et al.*, 1997a,b; Durell *et al.*, 1998).

However, the sequence-dependent elastic and structural properties of p53 response-elements has remained largely obscure, owing to the difficulties in visualizing the conformations of such short DNA fragments in solution with high precision. Nonetheless, T4 ligase-mediated cyclization (ring closure) has proved to be a powerful method for determining the curvature in protein-DNA complexes and the deformability of short DNA segments (Ulanovsky *et al.*, 1986; Zahn & Blattner,

1987; Lyubchenko *et al.*, 1991; Kahn & Crothers, 1992; Harrington, 1993). Using atomic force microscopy (AFM) imaging, we studied the conformation and elasticity of DNA microcircles obtained in this way which consisted of alternating phased poly A-tract and GGGCCC sequences (Han *et al.*, 1997). Subsequently, theoretical modeling was used to rationalize the Zn²⁺-induced structural transition in these microcircles on the basis of mechanical and elastic properties of the DNA polymer (Zhou & Ou-Yang, 1999a).

Here, we investigate, using the same approach, the mechanical and conformational properties of p53 response-element DNA derived from the *p21/waf1/cip1* gene promoter (Hartwell & Kastan, 1994; Balagurumorthy *et al.*, 1995; Nagaich *et al.*, 1997a). Upon ligation of 42 bp oligonucleotide duplexes containing *waf1/cip1/p21* half sites, a significant fraction of the linear ligamers formed circularize thermally in the absence of p53. Thus, the microcircles obtained are devoid of any structural alterations induced by p53 and the conformational properties observed must therefore be intrinsic to the p53 response-element DNA itself. We then employ MacMode AFM (Han *et al.*, 1996) to visualize in solution 168 bp microcircles produced from this ligation (4 × 42 bp precursors). We find that the *waf1/cip1/p21* microcircles are all markedly puckered in contrast to the planarity exhibited by the earlier A-tract/GGGCCC microcircles.

To interpret the puckering phenomenon, we have assumed that during ring closure the two ends of the *waf1/cip1/p21* DNA segment have twist mismatch, which would lead in the absence of writhe to a non-integral equilibrium linking number in the covalently closed microcircle. However, since the linking number of a covalently closed circular chain is required to be integral (White, 1969; Fuller, 1971, 1978; Crick, 1976), the effective linking number excess or deficit developed upon ring closure must be resolved by a change in writhe which destabilizes the planar configuration of the microcircle and causes it to pucker. We have performed quantitative calculations based on this mechanism and have found excellent agreement between theory and the experimental observations. Such a comparison suggests that the *waf1/cip1/p21* p53 response-element DNA sequence has an enhanced flexibility, and is intrinsically over-twisted. Such properties are likely to be shared by other p53-binding sequences and may be a determinant of the binding selectivity of the p53 tumor-suppressor protein to its various response-elements.

Theory

Measurement of degree of puckering

The degree of puckering in the microcircles was described by two quantities, the aspect ratio σ and the writhing number Wr . We defined a 3 × 3 symmetric coordinate tensor τ (Zhang, 2000):

$$\tau_{ij} = \frac{3 \int_0^L (r_i(s) - r_i^0)(r_j(s) - r_j^0) ds}{\int_0^L (\mathbf{r}(s) - \mathbf{r}^0)^2 ds} \quad (i, j = 1, 2, 3) \quad (1)$$

where $\mathbf{r}(s)$ denotes the axial vector of the DNA polymer along its arc length s , and $\mathbf{r}^0 = \int_0^L \mathbf{r}(s) ds / L$ is the center of mass of a DNA polymer of total contour length L ; $r_i(s)$ is the projection of the axial vector on the i th axis of the three-dimensional Cartesian coordinate system. The positive definite tensor τ , in fact, represents the configurational ellipsoid of a closed DNA microcircle; we can always find three mutually orthonormal directions (called the principal axes) as the new coordinate directions, with the tensor τ being diagonal in this principal coordinate system. Denote the three positive eigenvalues of equation (1) as T_1, T_2 and T_3 in the order $0 \leq T_1 \leq T_2 \leq T_3$ with $T_1 + T_2 + T_3 = 3$. T_i is proportional to the average squared projection of a DNA microcircle on the i th principal direction, i.e. the i th major axis of the configurational ellipsoid of the DNA microcircle.

For DNA microcircles obtained in our experiment, we found that the values for T_1 are always very small, indicating that the observed puckering could have been significantly reduced due to the adsorption of microcircles onto the surface, while T_3 is much greater than T_2 (see below). This kind of rectangular conformation of DNA microcircles can be more concisely signified by an aspect ratio σ :

$$\sigma = \sqrt{\frac{T_3}{T_1 + T_2}} \quad (2)$$

which represents the ratio of the projection of the molecule along its longest principal axis (corresponding to T_3) to that of the one perpendicular to this axis. Obviously, for a planar DNA circle $\sigma = 1$.

While the extent to which the overall contour of the DNA microcircles deviates from being circular is well characterized by its major axes and the aspect ratio, the extent to which it deviates from being planar is characterized by the writhing number Wr , which is defined by the following double integral along the closed contour of the molecule (White, 1969; Fuller, 1971):

$$Wr = \frac{1}{4\pi} \oint \oint \frac{d\mathbf{r}(s) \times d\mathbf{r}(s') \cdot [\mathbf{r}(s) - \mathbf{r}(s')]}{|\mathbf{r}(s) - \mathbf{r}(s')|^3} \quad (3)$$

The x , y and z coordinates of the polymer backbone were measured directly from images at n points along the DNA contour. When n is large enough (say $n = 30$), the integrations in equations (1) and (3) can be calculated as the sum of coordinates of the n number of points.

Elastic model of DNA microcircles

We model DNA microcircles as a closed elastic rod with bending and twisting rigidity constants B and C , respectively, and intrinsic twisting rate ω_0 (corresponding to the situation in which a relaxed DNA molecule is a right-handed double helix with a pitch of about 3.4 nm which contains about 10.5 base-pairs (Wang, 1979)). We define a moving orthonormal trihedral $\{\hat{\mathbf{e}}_1(s), \hat{\mathbf{e}}_2(s), \hat{\mathbf{e}}_3(s)\}$ along the DNA axial line $\mathbf{r}(s)$, with $\hat{\mathbf{e}}_3 = d\mathbf{r}/ds$ being the unit tangent vector to the axial line. The choices of the other two unit vectors $\hat{\mathbf{e}}_1$ and $\hat{\mathbf{e}}_2$ are arbitrary, as long as $\hat{\mathbf{e}}_1 \times \hat{\mathbf{e}}_2 = \hat{\mathbf{e}}_3$. Here, we may specify $\hat{\mathbf{e}}_1$ as pointing from the central line to one of the two backbones. For the convenience of subsequent calculations, we use Euler angles θ, ϕ and ψ to describe the directions of $\hat{\mathbf{e}}_i$, with $\hat{\mathbf{e}}_3 = \{\sin\phi\sin\theta, -\cos\phi\sin\theta, \cos\theta\}$ and $\hat{\mathbf{e}}_1 = \{\cos\phi\cos\psi - \sin\phi\sin\psi\cos\theta, \sin\phi\cos\psi + \cos\phi\sin\psi\cos\theta, \sin\psi\sin\theta\}$ (Landau & Lifshitz, 1976).

According to Hooke's law, the total deformation energy ε of the elastic rod, which is the sum of the bending curvature energy ε_B of the central axis and the twisting energy ε_T of the backbones winding around the central axis, i.e. $\varepsilon = \varepsilon_B + \varepsilon_T$ (Bouchiat & Mezard, 1998; Zhou & Ou-Yang, 1999a), can be written as:

$$\begin{aligned} \varepsilon_B &= \frac{B}{2} \int_0^L \left(\frac{d\hat{\mathbf{e}}_3}{ds} \right)^2 ds \\ &= \frac{B}{2} \int_0^L (\dot{\phi}^2 \sin^2 \theta + \dot{\theta}^2) ds \end{aligned} \quad (4)$$

and:

$$\begin{aligned} \varepsilon_T &= \frac{C}{2} \int_0^L \left(\hat{\mathbf{e}}_3 \times \hat{\mathbf{e}}_1 \cdot \frac{d\hat{\mathbf{e}}_1}{ds} - \omega_0 \right)^2 ds \\ &= \frac{C}{2} \int_0^L (\dot{\phi} \cos \theta + \dot{\psi} - \omega_0)^2 ds \end{aligned} \quad (5)$$

Here, $(\dot{\cdot})$ denotes the differentiation with respect to the arc length s of the DNA axis.

Puckered conformations are induced by excess linking number

The bending energy ε_B and the twisting energy ε_T are usually decoupled, since ε_B depends on local curvature of the central axis, while ε_T is the function of displacements of twist of the DNA base-pairs from the equilibrium positions. For a torsionally relaxed small loop (e.g. nicked DNA polymer), the torsional energy of DNA vanishes, and the DNA molecule has the minimum bending energy of a planar circle. The effective coupling between bending and torsional energies rises for covalently closed DNA polymers, since the number of times two strands of the DNA duplex are inter-wound, i.e. the linking number Lk , is a topological invariant. The planar

circle would no longer correspond to a stable minimum of the total elastic energy when the linking number deficit/excess is beyond a certain threshold value, which is a function of bending and torsional stiffness of the DNA polymer (Benham, 1989; Gutter & Leibler, 1992; see also below). In fact, the spatial configuration of a circular DNA depends upon the competition between bending and twist changes. Planar DNA microcircles will pucker if the decrease in torsional energy through changing the twist of the base-pairs exceeds the increase of bending energy caused by writhing of the polymer helical axis.

Mathematically, the topologically invariant linking number Lk of a circular DNA can be decomposed as the sum of two parts, the total writhing number Wr of the closed axial line and the twisting number Tw of one DNA backbone winding relative to the central axis, i.e. $Lk = Tw + Wr$ (White, 1969; Fuller, 1971, 1978; Crick, 1976). Using the above parameterization of Euler angles, the twist number can be written as:

$$\begin{aligned} Tw &= \frac{1}{2\pi} \int_0^L \hat{\mathbf{e}}_3 \times \hat{\mathbf{e}}_1 \cdot \frac{d\hat{\mathbf{e}}_1}{ds} \\ &= \frac{1}{2\pi} \int_0^L (\dot{\phi} \cos \theta + \dot{\psi}) ds \end{aligned} \quad (6)$$

and, for a slightly puckered DNA microcircle, the expression for the writhing number in equation (3) can be calculated alternatively by the following formula (Fuller, 1978):

$$\begin{aligned} Wr &= \frac{1}{2\pi} \int_0^L \frac{\hat{\mathbf{t}}_0 \times \hat{\mathbf{e}}_3 \cdot \hat{\mathbf{t}}_0 + \hat{\mathbf{e}}_3}{1 + \hat{\mathbf{t}}_0 \cdot \hat{\mathbf{e}}_3} ds = -\frac{1}{2\pi} \int_0^L \\ &\times \frac{\lambda \cos \theta + \dot{\phi} \sin \theta \cos \theta \cos(\phi - \lambda s) + \dot{\theta} \sin(\phi - \lambda s)}{1 + \sin \theta \cos(\phi - \lambda s)} ds \end{aligned} \quad (7)$$

where $\hat{\mathbf{t}}_0 = (\sin \lambda s, -\cos \lambda s, 0)$ ($\lambda = 2\pi/L$) is the tangent vector of an undeformed planar circle.

The stable conformation of circular DNA corresponds to that with a minimum of the total deformation energy ε , for a given linking number difference $\Delta Lk = Lk - Lk_0$ where $Lk_0 = \omega_0 L / 2\pi$, i.e. the equilibrium linking number of a relaxed DNA microcircle. Thus, the stable configuration, $\mathbf{r}(s)$, can be found by minimizing the elastic energy of the DNA microcircle. According to the detailed calculation in the next subsection, we find that the stable configuration is given by:

$$\begin{aligned} \bar{\mathbf{r}}(s) &= \int_0^s \hat{\mathbf{e}}_3(s') ds' \\ &= \left\{ \int_0^s (v \cos 2\pi s'/L \right. \\ &\quad + \sqrt{1 - v^2} \sin 2\pi s'/L) \sqrt{1 - u^2} ds' \\ &\quad \times \int_0^s (-\sqrt{1 - v^2} \cos 2\pi s'/L \\ &\quad \left. + v \sin 2\pi s'/L \sqrt{1 - u^2} ds', \int_0^s u ds' \right\} \end{aligned} \quad (8)$$

where:

$$\begin{aligned} u &= (m^2 - 1/4)^{-1/4} \\ &\quad |Wr|^{1/2} \sin(4m\pi s/L) \\ v &= \pm (1 - 1/4m^2)^{1/4} m^{-1/2} \\ &\quad |Wr|^{1/2} \cos(4m\pi s/L) \end{aligned} \quad (m = 1, 2, \dots) \quad (9)$$

Here, \pm correspond to positively and negatively writhed conformations, respectively.

The writhing number and the total deformation energy of the stable configuration is related to the linking number difference and rigidity constants as:

$$Wr = \Delta Lk - \text{sgn}(Wr) \sqrt{4m^2 - 1} B/C \quad (10)$$

$$\begin{aligned} \varepsilon &= \frac{2\pi^2}{L} [B + 2B \sqrt{4m^2 - 1} |Wr| \\ &\quad + C(\Delta Lk - Wr)^2] \end{aligned} \quad (11)$$

where $\text{sgn}(Wr) = 1$ for $Wr > 0$, and -1 if $Wr < 0$.

Equation (10) indicates that only when $|\Delta Lk| > \sqrt{3} B/C$ will a planar DNA microcircle become unstable. When this condition is satisfied but with $|\Delta Lk|$ still being small, the puckered configuration will be determined by equations (8), (9) and (10) with $m = 1$ because this yields the lowest deformation energy. Here, we consider the $m = 1$ case only.

Configuration of DNA loop of minimum deformation energy

The stable conformation of circular DNA can be deduced by minimizing the elastic deformation energy described by equations (4) and (5) under the constraint of fixed linking number deficit ΔLk .

Note that in equations (4) and (7), both the writhing number Wr and the bending energy ε_B depend only on $\hat{\mathbf{e}}_3$, the configuration of the central axis. To obtain the stable configuration corresponding to the minimum of the total deformation energy ε , we first minimize the bending and twisting energy at a fixed writhing number, and then minimize the resulting expression with respect to writhing number (Gutter & Leibler, 1992).

For given linking and writhing numbers, the minimum total twisting energy is easily obtained

from:

$$\varepsilon_T(Wr) = \frac{2\pi^2 C}{L} (\Delta Lk - Wr)^2 \quad (12)$$

To obtain the minimum of bending energy ε_B for a given writhing number, we perform the following expansions of the Euler angles:

$$\begin{aligned} \cos \theta(s) &= \sum_{m=1}^{\infty} (a_m \sin 2m\lambda s + b_m \cos 2m\lambda s) \\ \sin(\phi(s) - \lambda s) &= \sum_{m=1}^{\infty} (c_m \sin 2m\lambda s + d_m \cos 2m\lambda s) \end{aligned} \quad (13)$$

Here $\lambda = 2\pi/L$, and the coefficients a_m , b_m , c_m and d_m are all small quantities far less than unity. To ensure the ring-closure condition $\int_0^L \hat{e}_3(s) ds = 0$, in the above expansions only even deformation modes are kept. Then, to second order in the deformations, equation (7) leads to:

$$Wr = \sum_{m=1}^{\infty} m(a_m d_m - b_m c_m) \quad (14)$$

and equation (4):

$$\begin{aligned} \varepsilon_B &= \frac{2\pi^2 B}{L} + \sum_{m=1}^{\infty} \frac{\pi^2 B}{L} [(4m^2 - 1)a_m^2 \\ &+ (4m^2 - 1)b_m^2 + 4m^2 c_m^2 + 4m^2 d_m^2] \end{aligned} \quad (15)$$

With the minimization of equation (15) under the constraint of equation (14), we have:

$$\varepsilon_B(Wr) = \frac{2\pi^2 B}{L} + \frac{4\pi^2 B}{L} \sum_{m=1}^{\infty} \sqrt{4m^2 - 1} |Wr| \quad (16)$$

and the corresponding stable configuration is characterized by:

$$\begin{aligned} \cos \theta &= u_0 \sin(2m\lambda s + \theta_0) \\ \sin(\phi - \lambda s) &= \pm \frac{\sqrt{4m^2 - 1}}{2m} u_0 \cos(2m\lambda s + \theta_0) \end{aligned} \quad (17)$$

where θ_0 is an arbitrary constant and the deformation amplitude u_0 is determined by the writhing number from the following equation:

$$Wr = \pm \frac{\sqrt{4m^2 - 1}}{2} u_0^2 \quad (18)$$

Thus, with a simple minimization of the summation of equations (12) and (16) with respect to Wr , we can obtain the minimum deformation energy and corresponding stable configuration of the DNA microcircle; see equations (8-11).

Results and Discussion

DNA configuration and its degree of pucker

Images of the *waf1/cip1/p21* microcircles obtained on freshly cleaved 3-aminopropyltriethoxysilane (AP)-treated mica are shown in Figure 1(a) and at a higher magnification in Figure 1(b). The structures are not simple circles, but exhibit a ‘‘clover-leaf’’ shape. In addition, these microcircles were also imaged on $MgCl_2$ -treated mica (Han *et al.*, 1997) under identical conditions (Figure 1(c)) to examine possible influences of the surface and its modification on the structure. As evident from

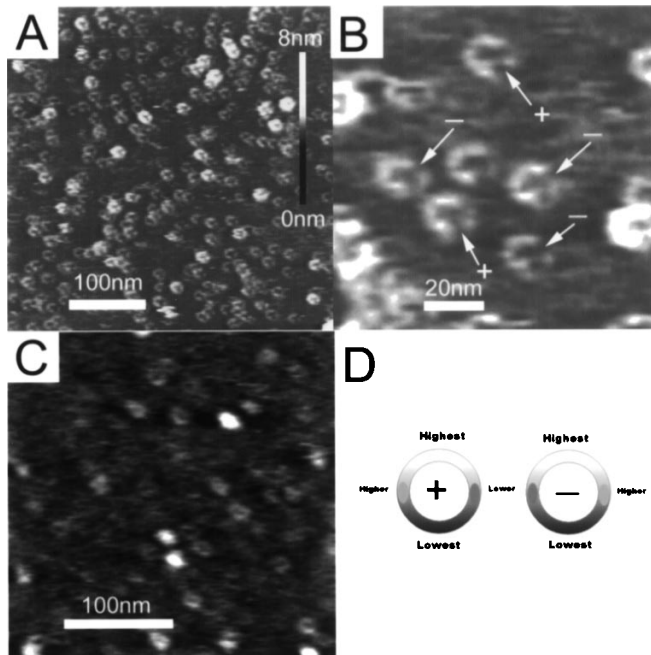


Figure 1. Typical MacMode AFM (Han *et al.*, 1996) images of DNA microcircles containing four *waf1/cip1/p21* p53 response-elements. (a) and (b) are the images obtained on AP-treated mica under 0.1 mM Tris-HCl (pH 8.0) at low and high magnifications, respectively. (c) images on $MgCl_2$ -treated mica. The x - y scale is shown by the horizontal bar and the height scale by the vertical bar. The circles have a ‘‘clover-leaf’’ appearance that was not seen in previous images obtained with uniformly bent A-tract DNA microcircles (Han *et al.*, 1997). In (b), positively and negatively writhed microcircles are indicated and the arrowhead points towards the lowest point along the contour. A schematic representation of the topological difference between these two conformers is shown in (d).

Figure 1(a) and (c), the overall shape and the conformational features observed in $MgCl_2$ were found to be essentially indistinguishable from those obtained with AP-treated surfaces. However, the resolution obtained for the *waf1/cip1/p21* microcircles in $MgCl_2$ is notably poorer compared to that of microcircles made up of phased A-tract/GGGCCC sequences (Han *et al.*, 1997). We attribute this to weaker adhesion of *waf1/cip1/p21* circles to the surface owing to their non-planar clover-leaf shape, compared to the topologically planar circles derived from alternating A-tract/GGGCCC sequences. From Figure 1(a) and (c) it can be seen that the images of *waf1/cip1/p21* circles on AP-treated mica surfaces are higher in resolution compared to the same circles on $MgCl_2$ -treated mica. We therefore decided to use the images obtained using AP-treated mica for the detailed analysis reported here.

The images collected both on AP and $MgCl_2$ -treated mica were quite stable from scan to scan and reproducibly much broader at certain points along the contour. This effect could be accounted for by the finite radius of the imaging tip if the broader points were also the highest points, and this is clearly the case as seen in the images. Nonetheless, the overall shape cannot be a tip or surface-induced artifact because the orientation of the features varies within a single scan and also such structural features were observed on mica modified by two different ways.

The puckered circles adopt a chair-like conformation with one highest point (cleft) opposite the lowest point (trough) and two arms of intermediate elevations between these positions facing each other. These two arms are not in a single plane, however; one is lower in space than the other. The

relative locations of these two arms of different elevations with respect to the cleft and trough in the clover-leaf conformation allows identification of two different conformers in the population of the microcircles. These are positively and negatively writhed and representative examples are indicated in Figure 1(b). The arrowhead points towards the lowest point (trough) along the contour, which is located opposite to the highest point (cleft). The subtle distinction between these two conformers is schematically represented in Figure 1(d). When going from the highest to the lowest point in a clockwise direction along the contour, if the lower arm is encountered, the conformer is positively writhed and *vice-versa*.

Figure 2(a) shows the second dimensional gel used to prepare 168 bp *waf1/cip1/p21* microcircles. The covalently closed 168 bp microcircles migrate as an elongated band rather than as a circular spot in the presence of chloroquine (50 $\mu g/ml$) indicating the possible occurrence of more than one species. DNA from this band was isolated, incubated in 100 $\mu g/ml$ chloroquine and analyzed on a non-denaturing 10% (w/v) polyacrylamide gel (Figure 2(b)) containing chloroquine (100 $\mu g/ml$). Under these conditions, the covalently closed 168 bp microcircles resolve into two distinct bands, supporting the existence of two topoisomers as visualized by AFM. Upon chloroquine intercalation and subsequent unwinding of the DNA, the positively writhed microcircles become more relaxed while the negatively writhed molecules become more negatively supercoiled. As a result, the difference in the absolute magnitude of writhe after the unwinding increases and the positively and negatively writhed microcircles can fully separate on the gel.

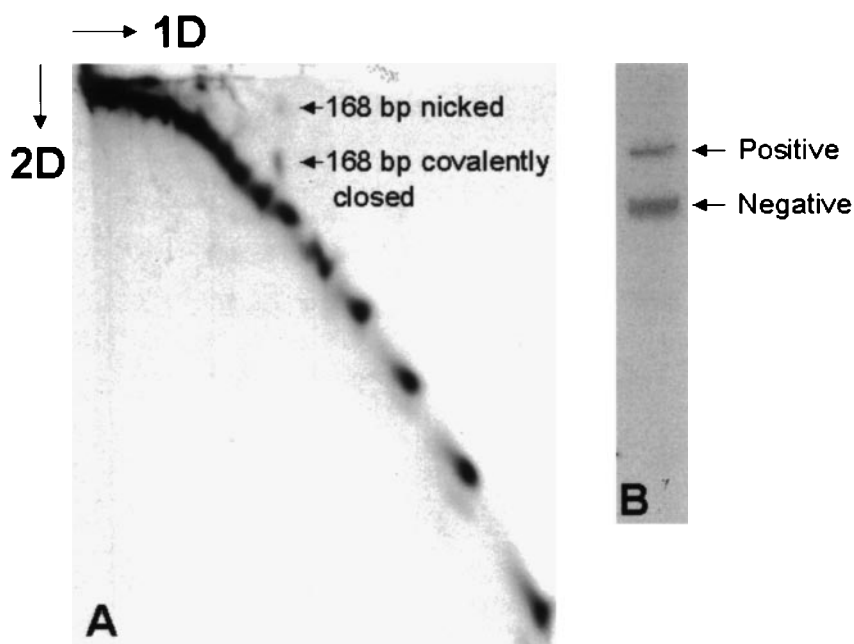


Figure 2. (a) Second dimensional polyacrylamide gel (8%) used to separate the *waf1/cip1/p21* microcircles from the linear and nicked circular ligamers. The upper row of spots are the nicked microcircles and the bottom diagonal contains the linear ligamers. The covalently closed microcircles appear as the middle row of spots. The first dimension was a 5% polyacrylamide gel. (b) Separation of positively and negatively writhed 168 bp microcircles on a 10% polyacrylamide gel. The gel, running buffer and the DNA sample contained chloroquine (100 $\mu g/ml$). The faster-moving band contains microcircles whose negative writhe has been increased by chloroquine intercalation, whereas the positively writhed molecules are more relaxed by chloroquine-induced unwinding and hence migrate more slowly.

The repeated structural motif is most easily seen if the path of the backbone is displayed in a three-dimensional plot. To do this we traced the height of 125 molecules as a function of contour length using special software developed for this purpose. Two representative traces are shown in Figure 3 (although all data were used in the calculations described below). The height variation along the contour is evident from the z-axis coordinates shown in nm. This structural motif is consistently observed in all the molecules, using data from four separate sets of runs using different AFM tips. It is clearly an intrinsic property of the molecules and not a consequence of the AFM tip geometry.

A total of about 125 images of individual microcircles were analyzed and the quantities characterizing the degree of pucker in these DNA configurations, namely the writhing number Wr , the eigenvalues of the tensor τ , and the aspect ratio σ , were calculated as defined by equations (1), (2) and (3). The average values are listed in Table 1. We noticed that all the 125 microcircles recorded are considerably puckered, either positively or negatively. The average (absolute) writhing number for the 125 microcircles is 0.108 ± 0.01 ; and the

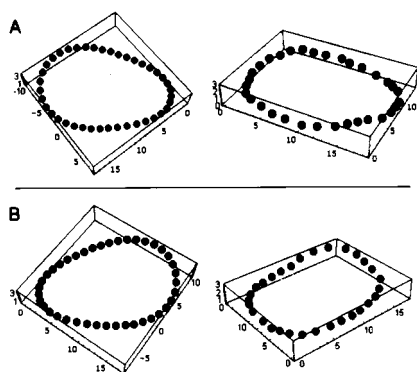


Figure 3. A comparison of measured (left column) and calculated (right column) contours of (a) positively writhed and (b) negatively writhed molecules. Plots are three-dimensional projections. The maximum vertical range out of the x - y plane is approximately 1 nm. In contrast, planar circles are flat to within the noise level on the images (≈ 0.2 nm, Han *et al.* 1997). Contours were measured by recording the x , y and z coordinates of the backbone from the images and removing the distortion caused by the greater broadening of the high points in the images. The calculated contours were derived as explained in the text (for $Wr = 0.109$ and -0.098) and are displayed here on the same x , y and z scales as the measured data. Positively writhed molecules have a “deckchair” shape most sharply curved at the lowest point, as seen in both theoretical and measured contours. Negatively writhed molecules have a similar shape but of the opposite orientation, with the low point somewhat blunter than the positively writhed molecules. Only two experimentally determined contours are shown here, but the shapes were almost identical for all the populations measured, as characterized by the standard deviations of the configurational parameters listed in Table 1.

average squared aspect ratio σ^2 of the molecules is 1.78 ± 0.03 , indicating that the planar projections of most of the microcircles recorded should be elliptic (Figure 1(a) and (b)). The microcircles also have a slightly greater tendency to pucker negatively than positively (negative *versus* positive writhing) and the average absolute writhing number of negatively puckered microcircles is slightly less than that of the positively puckered ones (Table 1). Important questions therefore are: what causes the DNA microcircles to pucker away from the planar circular conformation, and what can account for the slightly higher tendency towards negative puckering?

Puckering is induced by twist mismatch in the DNA microcircle

The *waf1/cip1/p21* microcircles were prepared by a T4 ligase-mediated cyclization reaction (see, e.g. Harrington, 1993). Linear *waf1/cip1/p21* oligonucleotides can move freely in solution, and when the two ends of each segment are sufficiently close to each other in correct spatial and rotational alignment, the T4 ligase can ligate them into a ring. The microcircles so formed were collected, religated (to ensure that random nicks were sealed) and isolated electrophoretically, as described in Materials and Methods. In previous work, it was shown that when a p53 tetramer binds to its DNA response element and bends the DNA axis, the twist in the double helix also increases (Nagaich *et al.*, 1999). We therefore suspected that the twisting deformations in the flexible *waf1/cip1/p21* response element should be an intrinsic property of the sequence itself (Zhou & Ou-Yang, 1998; Zhou *et al.*, 1999b). While the two sugar-phosphate strands of a straight *waf1/cip1/p21* segment of 168 bp wind around each other by precisely 16 turns (with a pitch of 10.5 bp), the twisting number of the curved *waf1/cip1/p21* double-helical DNA may be assumed to exceed 16. Therefore, twist mismatch between the two ends of the *waf1/cip1/p21* double-helix is anticipated to exist before ligation, i.e. the bent DNA double helix may have a pitch slightly less than 10.5 bp, with the equilibrium linking number of a nicked planar *waf1/cip1/p21* microcircle assuming a number slightly larger than 16. However, after ring closure and ligation of all nicks, the actual linking number of the microcircle is required to be an integer. Hence torsional stress is expected to develop in the closed microcircle, which destabilizes the planar configuration and induces puckering as the torsional stress is partly absorbed by writhing.

To check this point, negatively and positively puckered theoretical conformations with the same writhing numbers as listed in Table 1 were calculated according to the elastic rod model described in Theory. Figure 3(a) and (b) show, respectively, the calculated positively and negatively puckered microcircles with writhing number 0.108 and -0.098 (left column) as well as examples of exper-

Table 1. Configurational parameters of 168 bp DNA microcircles containing four *waf1/cip1/p21* p53 response-elements

Configuration	n	$\langle Wr \rangle$	$\langle T_1 \rangle$	$\langle T_2 \rangle$	$\langle T_3 \rangle$	$\langle \sigma^2 \rangle = \left\langle \frac{T_3}{T_1 + T_2} \right\rangle$
Negatively writhed	65	-0.098 ± 0.011	0.003 ± 0.0004	1.09 ± 0.02	1.91 ± 0.02	1.75 ± 0.04
Positively writhed	60	$+0.109 \pm 0.013$	0.003 ± 0.0004	1.07 ± 0.02	1.93 ± 0.02	1.80 ± 0.04
Summation	125	0.108 ± 0.01	0.003 ± 0.0003	1.08 ± 0.01	1.92 ± 0.01	1.78 ± 0.03

These parameters were obtained from the atomic force microscopy images of the microcircles in buffer. The average eigenvalues and aspect ratio are calculated separately for positively and negatively writhed circles.

imentally recorded configurations with positive and negative pucker (right column). The similarity between theory and experiment is striking, supporting the above puckering mechanism on the basis of over-twist in the *waf1/cip1/p21* response-element DNA.

To compare quantitatively the theoretical predictions with experimental observations, the structural parameters for the theoretical puckered DNA microcircles were calculated and are listed in Table 2. First, the experimentally determined average writhing number for positively and negatively supercoiled microcircles is used in equation (9); then the puckered conformation is determined by equation (8) and the parameters T_i are obtained as the eigenvalues of the ellipsoid tensor equation (1). The writhing number of the theoretical configuration has been recalculated by equation (3) to ensure consistency. It should be noted that the DNA microcircles are not "free" in solution, but rather are adsorbed to an atomically flat surface when they are scanned by AFM. The attachment to a surface should reduce the degree of pucker from its normal value in solution. This point evidently manifests itself in the difference between the experimental value of the major axis T_1 and the theoretical calculation; the former is smaller than the latter, although both are much less than unity (Tables 1 and 2). However, the theoretical values of other "untainted" conformational parameters T_2 , T_3 and σ of both positively and negatively puckered conformations are in good agreement with the experimental values. These coincidences give support to our interpretation that the puckering of *waf1/cip1/p21* microcircles is caused by twist mismatch prior to ring closure and that the discrepancy between the theoretical and experimental T_1 values is not a serious limitation to this method in quantifying the degree of over-twist causing the experimentally observed writhe in the *waf1/cip1/p21* microcircles.

Estimations of twist mismatch and bending rigidity for the *waf1/cip1/p21* sequence

The theoretical approach described here makes it possible to estimate the extent of twist mismatch as well as the flexibility of the *waf1/cip1/p21* DNA response-element sequence from the magnitude of the average writhing number for the puckered conformations. The earlier phasing studies estimated that binding of p53DBD over-twists each response-element by about 35° on average, while binding of wild-type p53 over-twists it by about 70° (Nagaich *et al.*, 1999). Thus, in the present case of four response-element repeats, the total over-twisting should lie in the range 140° to 280° , far less than one full turn (360°).

A linear 168 bp DNA fragment containing four *waf1/cip1/p21* response-elements has a twisting number precisely equal to 16. We assume that during bending to form a microcircle, bending-twisting coupling causes this DNA segment to have an equilibrium twist number $16 + x$ (with $0 < x < 1$) and hence the effective equilibrium linking number $Lk_0 = 16 + x$ (because the torsionally relaxed DNA microcircle will be planar). After ring closure, however, the linking number Lk of the microcircle must be an integer.

In principle, the linking number of the randomly ligated DNA circle might assume different integral values due to thermal fluctuations. Analysis of equilibrium populations of topoisomers, obtained by either the ligation of nicked circles (Depew & Wang, 1975) or the treatment of covalently closed circles with an appropriate DNA topoisomerase (Pulleyblank *et al.*, 1975), has shown that the distribution in the linking number Lk of the randomly ligated DNA rings is gaussian, centered at the equilibrium linking number Lk_0 of the relaxed DNA double-helix, i.e.:

$$P(Lk) \approx \exp[-K(Lk - Lk_0)]^2 \quad (19)$$

Table 2. Configurational parameters of DNA microcircles calculated by the elastic rod model

Configuration	Wr	T_1	T_2	T_3	$\sigma^2 = \frac{T_3}{T_1 + T_2}$
Negatively writhed	-0.098	0.045	1.042	1.913	1.76
Positively writhed	0.109	0.051	1.015	1.934	1.81

The experimental values of writhing numbers from Table 1 are the input for the theoretical calculations.

where K is a DNA length-dependent proportionality constant. For DNA segments of length less than 210 bp, K is greater than 18.6 according to the ligation experiment of Horowitz & Wang (1984). Thus, the distribution of topoisomers of 168 bp microcircles is sharply peaked around Lk_0 ; that is, the integral value of Lk equals 16 or 17. The relative frequency of other values of Lk is in fact unobservable (less than 10^{-16} according to equation 19).

If $Lk = 16$, then compared to its equilibrium value, the microcircle is negatively writhed and has a deficit linking number $\Delta Lk^- = -x$; on the other hand, if $Lk = 17$, then it is positively writhed and has $\Delta Lk^+ = 1 - x$. Since we know from Table 1 that the negatively supercoiled configurations have an average writhing number $Wr^- = -0.098$ and the positive ones have an average writhing number $Wr^+ = 0.109$, we can derive from equation (10) that:

$$Wr^+ + Wr^- = \Delta Lk^+ + \Delta Lk^- = 1 - 2x \quad (20)$$

and obtain $x = 0.4945$. This value means that after the 168 bp linear DNA fragment is closed into a microcircle, the DNA molecule is over-twisted by $0.4945 \times 360^\circ = 178^\circ$, i.e. 44.5° for each precursor oligonucleotide containing a 20 bp *waf1/cip1/p21* repeat. This value lies between the previously reported values of 35° and 70° obtained by phasing experiments using p53DBD and wild-type p53, respectively (Nagaich *et al.*, 1999). The above estimate also suggests that $|\Delta Lk^-|$ is slightly less than ΔLk^+ . Therefore, equation (11) indicates that the total deformation energy for the negative puckering is slightly less than that for the positive puckering, accounting for the observed small excess of negatively puckered circles.

The present work confirms the idea that p53 consensus sequences have enhanced flexibility (Balagurumoorthy *et al.*, 1995). Equation (10) indicates that for the *waf1/cip1/p21* consensus sequence, the ratio of bending rigidity versus twisting rigidity is:

$$\frac{B}{C} = (\Delta Lk^+ - Wr^+)/\sqrt{3} = 0.23 \quad (21)$$

If we take the twisting persistence length $C/k_B T$ to be 75 nm, as suggested by the experimental work of Horowitz & Wang (1984), then equation (21) predicts the bending persistence length of the *waf1/cip1/p21* sequence to be $l_p = B/k_B T = 17$ nm, only one-third of the effective value of 53 nm for the long DNA molecules determined by force-extension experiments (Bustamante *et al.*, 1994). Thus, the *waf1/cip1/p21* sequence seems to be extremely flexible compared to a random DNA sequence. The locus of this enhanced flexibility is probably in the flexible junction CA(TG) at the dyad of each *waf1/cip1/p21* half binding decamer as suggested by molecular modeling studies (Nagaich *et al.*, 1997a, 1999; Durell *et al.*, 1998). Additional evidence for

this will be presented elsewhere. From the present experiments, the reverse possibility cannot be entirely ruled out, namely that the bending rigidity $B/k_B T \cong 53$ nm but the twisting rigidity is extremely large in the *waf1/cip1/p21* double-helix compared to random DNA sequence. However, if this is the case, equation (21) requires that $C/k_B T \cong 230$ nm to reproduce the observed microcircle puckering. Experiments seem to favor the first interpretation since (i) p53 tetramers can both bend and over-twist the DNA double helix without much difficulty, indicating both its flexibility and moderate twisting rigidity (Nagaich *et al.*, 1999) and (ii) as the present work demonstrates, short *waf1/cip1/p21* response-element-containing sequences are flexible enough to form microcircles as small as 168 bp driven only by thermal energy.

The results presented here show clearly that microcircle formation by the *waf1/cip1/p21* response-element DNA in the absence of p53 can be attributed to its intrinsic flexibility/bendability and the writhe/puckering introduced upon ring closure is due to the over-twist in the DNA prior to ligation, as predicted by the theoretical approach used here. These conclusions deduced for the naked p53 response-element DNA might have important ramifications in the light of the coupling observed between the bending and twisting in the *waf1/cip1/p21* response-element DNA complexed with p53 as suggested by modeling (Nagaich *et al.*, 1997a; Durell *et al.*, 1998) and implicit in the results of phasing experiments (Nagaich *et al.*, 1999). The over-twisting of DNA induced by p53 may be interpreted in the following way: upon p53 binding, the response-element is bent because of the steric requirements of the bound p53. The coupling between bending and twisting in turn leads to an increase in the overall twisting number. Recent electron-microscopy studies carried out by Cheney *et al.* (1999) demonstrated that, on average, wild-type p53 bends each DNA response-element by 40° - 48° , whereas p53DBD bends the response-element by 35° - 37° . These results, in conjunction with the phasing experiments of Nagaich *et al.* (1999), suggest a positive correlation between the bending and twisting of DNA in the tetrameric p53 nucleoprotein complex, consistent with the conformational properties (flexibility and over-twist) observed here for the free *waf1/cip1/p21* response-element DNA.

The occurrence of over-twist, in addition to the flexibility in the p53 response-element DNA, may represent a structural mechanism by which p53 can selectively bind to its response-elements in the genome. This may also allow the control of DNA binding by local supercoiling effects in promoter regions of genes. In this connection, torsional rigidity measurements by Selvin *et al.* (1992) showed that positively supercoiled DNA is more anisotropically flexible than the negatively supercoiled DNA and hence torsional rigidity might play a role in protein binding to the DNA.

Conclusions

Here, we have prepared DNA microcircles made up of tandem repeats of precursor sequences containing the p53 binding element *waf1/cip1/p21* using T4 DNA ligase-mediated cyclization and have observed their conformations by AFM in solution. The *waf1/cip1/p21* microcircles are remarkably puckered with armchair-like conformations. The mechanism proposed here suggests that the puckering is caused by twist mismatch in bent DNA microcircles. Our theoretically obtained puckered conformations are in close quantitative agreement with experimental observations, indicating that the *waf1/cip1/p21* response-element possesses an enhanced flexibility and a unique ability to over-twist by 44.5°. This is in reasonable agreement with earlier estimates of p53-induced over-twisting by other methods. We suggest that the methodology we have used to decipher the intrinsic structural deformations in the p53 response-element DNA can be employed as a more general method to decode the structural information in the other DNA transcription factor binding sequences.

It is likely that the novel elastic properties intrinsic to the *waf1/cip1/p21* response-element DNA reported here could be important for p53 recognition and the control of DNA binding in promoter regions. Since the general design of all p53 response-elements is similar (Durell *et al.*, 1998; Olson *et al.*, 1998), these structural properties may be shared by other p53 response-elements as well and may represent a powerful discriminatory mechanism by which p53 DNA-binding properties, and hence p53 function, may be controlled at the promoter level.

Materials and Methods

Microcircles

The following 42 base-pair sequence was used in all ligations. It contains repeats of the binding half site for the biologically important regulatory protein p53, derived from the *p21/waf1/cip1* promoter (Hartwell & Kastan, 1994):

```
5' TCCGATGAACATGTCCATGAATTAATCAACATGTTGGGCCTT 3'
3' TACTTGTACAGGTACTTAATTAGTGTACACCCGAAAGGC 5'
```

The p53 half site is displayed in bold type and is believed to be the locus of enhanced flexibility (Durell *et al.*, 1998; Nagaich *et al.*, 1999). Two oligodeoxyribonucleotides 42 bases in length were synthesized, purified and annealed to provide sticky ends of four bases. This duplex was used as a precursor in T4 ligase-mediated cyclization experiments (Ulanovsky *et al.*, 1986; Lyubchenko *et al.*, 1991; Harrington, 1993; Balagurumorthy *et al.*, 1995) to produce the DNA microcircles studied here. The 168 bp DNA microcircles were eluted from the second dimension polyacrylamide gel (Figure 2(a)) as described (Balagurumorthy *et al.*, 1995), in 0.5 M ammonium acetate, 10 mM magnesium acetate, 1 mM

EDTA (pH 8.0) and 0.1% (w/v) SDS. The gel-eluted DNA was precipitated with two volumes of ethanol at 4°C and dried. For AFM imaging, the DNA was passed through a NAP-10 (Pharmacia) column equilibrated with freshly distilled water. The desalted circular DNA was concentrated in a Speed Vac (Savant) and dissolved in 0.1 mM Tris-HCl (pH 8.0). DNA solutions and buffers for AFM imaging were prepared with 17/18 MΩ water from a Nanopure water-purification system (Barnstead, Iowa). For the gel analysis of 168 bp microcircles, the ethanol-precipitated DNA was incubated in 10 mM Tris-HCl (pH 8.0), 1 mM EDTA and 100 µg/ml chloroquine for 30 minutes and run on a 10% polyacrylamide gel in 1 × TBE (90 mM Tris-Borate, 2 mM EDTA) containing 100 µg/ml of chloroquine.

Modification of mica and sample deposition

The 3-aminopropyltriethoxysilane (APTES; 98% pure; Sigma Chemical Co., St Louis, MO) was distilled under vacuum prior to use. Mica surfaces were treated for five minutes with a 10 µl suspension containing one part of APTES and 10,000 parts of water. They were then rinsed with 200 µl of water and dried with filtered argon. This method differs from the modification of mica by APTES in vapor phase used conventionally (Lyubchenko *et al.*, 1996). An alternative mica surface was also prepared by rinsing freshly cleaved mica with 200 µl of 1 mM MgCl₂ as described by Han *et al.* (1997).

The AFM liquid cell (Molecular Imaging, Phoenix) was clamped over the APTES-modified mica on a MacMode sample plate and 300 µl of 168 bp microcircular DNA (0.5 µg/ml) in 0.1 mM Tris-HCl (pH 8.0) was added to the liquid cell. The DNA solution was allowed to stand over mica for at least ten minutes at ambient temperature before scanning. The DNA solutions used for imaging over MgCl₂-modified mica contained 1 mM MgCl₂.

AFM imaging

AFM imaging was done using a Pico APM from Molecular Imaging (Phoenix, AZ). Images were obtained with a magnetic AC drive (MacMode) using silicon MAClevers of nominal spring constant 0.6 N/m. The free operating amplitude was set at 5 nm p/p with a 10% reduction set-point. The drive frequency was 25 kHz. Images were saved in TIF format and analyzed using NIH Image software. The height scale was, in turn, calibrated using images of a 1 micron calibration grating (Silicon NDT, Moscow). Data for height as a function of tile position along the molecular contour were obtained by measuring the calibrated pixel density at selected points along the molecular contour using special software developed for this purpose.

Acknowledgments

Numerical calculations were performed at ITP-Net and at a PC donated to Y.Z. by the Alexander von Humboldt Foundation. Support of the experimental work at Arizona State University by NIH research grants CA 70274 and GM 553517 (R.E.H.) is gratefully acknowledged. The authors also acknowledge support from Molecular Imaging, Inc. (Phoenix, Arizona, USA) in the development of the MacMode AFM technology used in

the experimental parts of this work and express their thanks to Dr Judy Zhu of Molecular Imaging, Inc. for sharing her AP mica technology with us. The authors are grateful to Drs Ilga Winicov and Victor Zhurkin for many helpful and stimulating discussions.

References

- Balagurumorthy, P., Sakamoto, H., Lewis, M. S., Zambrano, N., Clore, G. M., Gronenborn, A. M., Appella, E. & Harrington, R. E. (1995). Four p53 DNA-binding domain peptides bind natural p53-response-elements and bend the DNA. *Proc. Natl Acad. Sci. USA*, **92**, 8591-8595.
- Benham, C. (1989). Onset of writhing in circular elastic polymers. *Phys. Rev. ser. A*, **39**, 2582-2586.
- Bewley, C. A., Gronenborn, A. M. & Clore, G. M. (1998). Minor groove-binding architectural proteins: structure, function and DNA recognition. *Annu. Rev. Biophys. Biomol. Struct.* **27**, 105-131.
- Bouchiat, C. & Mezard, M. (1998). Elasticity model of a supercoiled DNA molecule. *Phys. Rev. Letters*, **80**, 1556-1559.
- Bustamante, C., Marko, J. F., Siggia, E. D. & Smith, S. (1994). Entropic elasticity of λ -phage DNA. *Science*, **265**, 1599-1600.
- Cherny, D. I., Striker, G., Subramaniam, V., Jett, S. D., Palecek, E. & Jovin, T. M. (1999). DNA bending due to specific p53 and p53 core domain-DNA interactions visualized by electron microscopy. *J. Mol. Biol.* **294**, 1015-1026.
- Cho, Y., Gorina, S., Jeffrey, P. D. & Pavlitch, N. P. (1994). Crystal structure of a p53 tumor suppressor-DNA complex: understanding tumorigenic mutations. *Science*, **265**, 346-355.
- Crick, F. H. C. (1976). Linking numbers and nucleosomes. *Proc. Natl Acad. Sci. USA*, **73**, 2639-2643.
- Depew, R. E. & Wang, J. C. (1975). Conformational fluctuations of DNA helix. *Proc. Natl Acad. Sci. USA*, **72**, 4275-4279.
- Ding, H. F. & Fisher, D. E. (1998). Mechanisms of p53-mediated apoptosis. *Crit. Rev. Oncog.* **9**, 83-98.
- Durell, S. R., Appella, E., Nagaich, A. K., Harrington, R. E., Jernigan, R. L. & Zhurkin, V. B. (1998). DNA bending induced by tetrameric binding of the tumor-suppressor p53 protein: steric constraints on conformation. In *Structure, Motion, Interaction and Expression of Biological Macromolecules. Proceedings of the Tenth Conversation* (Sarma, R. H. & Sarma, H., eds), pp. 277-295, Adenine Press, Schenectady, NY.
- El-Deiry, W. S., Kern, S. E., Pietenpol, J. A., Kinzler, K. W. & Vogelstein, B. (1992). Definition of a consensus binding site for p53. *Nature Genet.* **1**, 45-49.
- ElHassan, M. A. & Calladine, C. R. (1996). Structural mechanics of bent DNA. *Endeavour*, **20**, 61-67.
- Friedman, P. N., Chen, X., Bargonetti, J. & Prives, C. (1993). The p53 protein is an unusually shaped tetramer that binds directly to DNA. *Proc. Natl Acad. Sci. USA*, **90**, 3319-3323.
- Fuller, F. B. (1971). The writhing number of a space curve. *Proc. Natl. Acad. Sci. USA*, **68**, 815-819.
- Fuller, F. B. (1978). Decomposition of the linking number of a closed ribbon. *Proc. Natl Acad. Sci. USA*, **75**, 3557-3561.
- Gutter, E. & Leibler, S. (1992). On supercoiling instability in closed DNA. *Europhys. Letters*, **17**, 643-648.
- Han, W. H., Lindsay, S. M. & Jing, T. (1996). A magnetically driven oscillating probe microscope for operation in liquids. *Appl. Phys. Letters*, **69**, 4111-4114.
- Han, W. H., Dlakic, M., Zhu, Y. W., Lindsay, S. M. & Harrington, R. E. (1997). Strained DNA is kinked by low concentrations of Zn^{2+} . *Proc. Natl Acad. Sci. USA*, **94**, 10565-10570.
- Harrington, R. E. (1992). DNA curving and bending in protein-DNA recognition. *Mol. Microbiol.* **6**, 2549-2555.
- Harrington, R. E. (1993). Studies of DNA bending and flexibility using gel electrophoresis. *Electrophoresis*, **14**, 732-746.
- Hartwell, L. H. & Kastan, M. B. (1994). Cell cycle control and cancer. *Science*, **266**, 1821-1828.
- Horowitz, D. S. & Wang, J. C. (1984). Torsional rigidity of DNA and length dependence of the free energy of DNA supercoiling. *J. Mol. Biol.* **173**, 75-91.
- Jett, S. D., Cherny, D. I., Subramaniam, V. & Jovin, T. M. (2000). Scanning force microscopy of the complexes of p53 core domain with supercoiled DNA. *J. Mol. Biol.* **299**, 585-592.
- Kahn, J. D. & Crothers, D. M. (1992). Protein induced bending and DNA cyclization. *Proc. Natl Acad. Sci. USA*, **89**, 6343-6347.
- Kern, S. E., Kinzler, K. W., Bruskin, A., Jarosz, D., Friedman, P., Prives, C. & Vogelstein, B. (1991). Identification of p53 as a sequence specific DNA-binding protein. *Science*, **252**, 1708-1711.
- Ko, L. J. & Prives, C. (1996). p53: puzzle and paradigm. *Genes Dev.* **10**, 1054-1072.
- Landau, L. D. & Lifshitz, E. M. (1976). *Mechanics*, 3rd edit., pp. 110-111, Pergamon Press, Oxford.
- Levine, A. J. (1997). p53, the cellular gatekeeper for growth and division. *Cell*, **88**, 323-331.
- Lyubchenko, Y. L., Shlyakhtenko, L. S., Chernov, B. & Harrington, R. E. (1991). DNA bending induced by cro protein binding as demonstrated by gel electrophoresis. *Proc. Natl Acad. Sci. USA*, **88**, 5331-5334.
- Lyubchenko, Y. L., Blankenship, R. E., Gall, A. A., Lindsay, S. M., Thiemann, O., Simpson, L. & Shlyakhtenko, L. S. (1996). Atomic force microscopy of DNA, nucleoproteins and cellular complexes: the use of functionalized substrates. *Scanning Microsc. Suppl.* **10**, 97-107.
- McNamara, P. T., Bolshoy, A., Trifonov, E. N. & Harrington, R. E. (1990). Sequence-dependent kinks induced in curved DNA. *J. Biomol. Struct. Dynam.* **8**, 529-538.
- Nagaich, A. K., Bhattacharyya, D., Brahmachari, S. K. & Bansal, M. (1994). A CA/TG sequence at the 5' end of oligo (A)-tracts strongly modulates DNA curvature. *J. Biol. Chem.* **269**, 7824-7833.
- Nagaich, A. K., Zhurkin, V. B., Sakamoto, H., Gorin, A. A., Clore, G. M., Gronenborn, A. M., Appella, E. & Harrington, R. E. (1997a). Architectural accommodation in the complex of four p53 DNA binding domain peptides with *p21/waf1/cip1* DNA response element. *J. Biol. Chem.* **272**, 14830-14841.
- Nagaich, A. K., Appella, E. & Harrington, R. E. (1997b). DNA bending is essential for the site-specific recognition of DNA response elements by the DNA binding domain of the tumor suppressor protein p53. *J. Biol. Chem.* **272**, 14842-14849.
- Nagaich, A. K., Zhurkin, V. B., Durell, S. R., Jernigan, R. L., Appella, E. & Harrington, R. E. (1999). p53 induced DNA bending and twisting: p53 tetramer binds on the outer side of a DNA loop and

- increases DNA twisting. *Proc. Natl Acad. Sci. USA*, **96**, 1875-1880.
- Olson, W. K., Gorin, A. A., Lu, X.-J., Hock, L. M. & Zhurkin, V. B. (1998). DNA sequence dependent deformability deduced from protein-DNA crystal complexes. *Proc. Natl Acad. Sci. USA*, **95**, 11163-11168.
- Pavletich, N. P., Chambers, K. A. & Pabo, C. O. (1993). The DNA-binding domain of p53 contains the four conserved regions and the major mutation hot spots. *Genes Dev.* **7**, 2556-2564.
- Pulleyblank, D. E., Shure, M., Tang, D., Vinograd, J. & Vosberg, H. P. (1975). Action of nicking-closing enzyme on supercoiled and nonsupercoiled closed circular DNA: formation of a Boltzmann distribution of topological isomers. *Proc. Natl Acad. Sci. USA*, **72**, 4280-4284.
- Schultz, S. C., Shields, C. C. & Steitz, T. A. (1991). Crystal structure of a CAP-DNA complex: the DNA is bent by 90°. *Science*, **253**, 1001-1007.
- Selvin, P. R., Cook, D. N., Pon, N. G., Bauer, W. R., Klein, M. P. & Hearst, J. E. (1992). Torsional rigidity of positively and negatively supercoiled DNA. *Science*, **255**, 82-85.
- Steitz, T. A. (1990). Structural studies of protein-nucleic acid interaction: the sources of sequence-specific binding. *Quart. Rev. Biophys.* **23**, 205-280.
- Stenger, J. E., Tegtmeyer, P., Mayr, G. A., Reed, M., Wang, Y., Wang, P., Hough, P. V. & Mastrangelo, I. A. (1994). p53 oligomerization and DNA looping are linked with transcriptional activation. *EMBO J.* **13**, 6011-6020.
- Tokino, T., Thiagalingam, S., El-Deiry, W. S., Wladman, T., Kinzler, K. W. & Vogelstein, B. (1994). p53 tagged sites from human genomic DNA. *Hum. Mol. Genet.* **3**, 1537-1542.
- Ulanovsky, L., Bodner, M., Trifonov, E. N. & Choder, M. (1986). Curved DNA: design, synthesis and circularization. *Proc. Natl Acad. Sci. USA*, **83**, 862-866.
- Wang, J. C. (1979). Helical repeat of DNA in solution. *Proc. Natl Acad. Sci. USA*, **76**, 200-203.
- Werner, M. H., Gornenborn, A. M. & Clore, G. M. (1996). Intercalation, DNA kinking and the control of transcription. *Science*, **271**, 778-784.
- White, J. H. (1969). Self-linking and Gauss integral in higher dimensions. *Am. J. Math.* **91**, 693-728.
- Zahn, K. & Blattner, F. R. (1987). Direct evidence for DNA bending at lambda replication origin. *Science*, **236**, 416-422.
- Zhang, Y. (2000). New approaches of the Monte Carlo calculation to the buckling of supercoiled DNA. *Phys. Rev. E.* **62**, R5923-R5926.
- Zhou, H. J. & Ou-Yang, Z.-C. (1998). Bending and twisting elasticity: a revised Marko-Siggia model on DNA chirality. *Phys. Rev. ser. E*, **58**, 4816-4819.
- Zhou, H. J. & Ou-Yang, Z. C. (1999a). Spontaneous curvature-induced dynamical instability of Kirchhoff filaments: application to DNA kink deformations. *J. Chem. Phys.* **110**, 1247-1251.
- Zhou, H. J., Zhang, Y. & Ou-Yang, Z.-C. (1999b). Bending and base stacking interactions in double-stranded DNA. *Phys. Rev. Letters*, **82**, 4560-4563.

Edited by I. Tinoco

(Received 24 July 2000; received in revised form 30 November 2000; accepted 30 November 2000)